Korean J. Chem. Eng., 39(7), 1891-1901 (2022)
DOI: 10.1007/s11814-022-1116-1

pISSN: 0256-1115
eISSN: 1975-7220

Extraction and phase transformation of iron in fine-grained complex hematite ore by suspension magnetizing roasting and magnetic separation

Shuai Yuan*,, Ruofeng Wang*,**, Qi Zhang*,**,†, Yanjun Li*,**, and Peng Gao*,****

*School of Resources and Civil Engineering, Northeastern University, Shenyang 110819, P. R. China
**National-Local Joint Engineering Research Center of High-efficient Exploitation Technology for Refractory Iron Ore Resources, Shenyang 110819, P. R. China
(*Received 2 August 2021 • Revised 28 January 2022 • Accepted 15 March 2022*)

Abstract−Suspension magnetizing roasting-magnetic separation technology was used to extract iron from fine-grained complex hematite ore. The effect of roasting conditions on the magnetizing roasting-magnetic separation process was studied. In summary, a concentrate with TFe grade of 69.96% and Fe recovery of 79.02% could be obtained under conditions of a roasting temperature of 500 °C, roasting time was 12 min, reductant concentration of 30%, and total gas flow of 200 mL/min, while TFe grade of final tailings was 5.66%. The phase composition and X-ray photoelectron spectroscopy analysis showed that hematite in the sample was transformed into magnetite during suspension magnetization roasting. After roasting, the proportion of Fe content in the phase of the magnetite increased from 5.91% in roasting feed to 97.96% in the roasting product. Transmission electron microscopy results also confirmed that hematite was transformed into magnetite with spinel structure, and the newly formed magnetite had good crystallinity. Scanning electron microscopy and BET analysis showed that roasting could increase the specific surface area, total pore volume, and porosity of the roasted product, which would strengthen the internal diffusion of CO and CO_2 in the particles, to improve the reduction rate of hematite. The loose internal structure of roasted particles led to the decrease of mechanical properties, which was conducive to improving the subsequent grinding efficiency.

Keywords: Refractory Iron Ore, Suspension Magnetization Roasting, Phase Selective Transition, Magnetic Performance, Microstructure Analysis

INTRODUCTION

Iron ore is a major raw material for the steel industry. The rapid growth of steel demand has put pressure on the resources reserves of iron ore in China. China's pig iron production is forecasted to be 0.87 billion tons in 2021, requiring the consumption of 1.38 billion tons of iron ore (TFe=62%), of which 1.14 billion tons of iron ore will be imported. China has abundant iron ore resources, but high-quality iron ore reserves are lacking and are increasingly depleted. The average Fe grade of China's iron ore is only 26.62% in 2019, down nearly 4 percentage points from 2011. Simultaneously, China's strict environmental protection policy leads the steel industry will continue to favor high-grade iron ore resources in the future, and foreign dependence on iron ore will remain high in the long term. The China Scrap Steel Association indicates that the proportion of scrap steel applied by Chinese steel companies has increased significantly, but it is still at a low level in the world (20.2% scrap ratio). Therefore, scrap steel is hardly an important weight to reduce the dependence on overseas iron ore in the short term. Considering the contradiction between the gradual depletion of domestic high-grade iron ore and the increasing demand for high-quality iron ore in the steel industry, it is particularly important in the efficient utilization of low-grade complex iron ore and tailings [1-5].

Low-grade iron ore with huge reserves requires specific beneficiation and metallurgical processes to meet the quality requirements of the iron and steel industry. A variety of beneficiation techniques including washing, jigging, spiral chute, shaking table, magnetic separation, and flotation are often used in combination to improve the quality of iron ore [6-15]. However, enrichment and recovery of iron minerals from fine-grained embedded iron ores is indeed a challenging task. To overcome the shortage of iron ore and meet the demand for steel production, efficient utilization of fine-grained iron ore by developing alternative beneficiation technologies is desirable [16]. The low-grade iron ore with fine-grained embedded has weak magnetic properties and poor floatability, so it is difficult to obtain good indexes by physical beneficiation methods such as gravity separation, magnetic separation, flotation, and even multiple combined beneficiation methods, the concentrate grade after beneficiation is difficult to reach more than 60%.

Pretreatment techniques such as high-voltage pulse discharge (HVPD), microwave treatment, and roasting can weaken the bond between minerals and vein particles and enhance the recovery of valuable metals from difficult to treat ores [17-20]. HVPD and microwaves lead to the separation of mineral interfaces between iron minerals with high conductivity/magnetic permeability (magnetite, hematite, etc.) and gangue minerals with low conductivity/magnetic permeability (quartz, etc.), thus promoting the monolithic dissociation of iron mineral particles [21-23]. Reduction roasting can

†To whom correspondence should be addressed.
E-mail: neuzhangqi@163.com

Table 1. Major chemical composition analysis of the sample

Composition	TFe	FeO	SiO_2	Al_2O_3	CaO	MgO	P	S	LOI
Content (wt%)	21.18	0.35	67.68	0.15	0.24	0.25	0.011	0.003	0.53

Table 2. Iron phase compositions of the sample

Iron phases	Fe in carbonate	Fe in magnetite	Fe in hematite	Fe in sulfide	Fe in silicate	Total
Content (wt%)	0.97	0.15	17.90	0.03	2.61	21.18
Percentage (%)	4.48	0.69	82.64	0.14	12.05	100.00

reduce the weakly magnetic iron minerals, such as hematite, goethite, and specularite, in iron ore to strongly magnetic magnetite, which is subsequently recovered by low-intensity magnetic separation [5, 24]. Sun et al. [3] described a method to recover iron minerals by the reduction roasting - magnetic separation process using iron tailings as raw material. The influence of process parameters on the magnetic concentrate was investigated, and concentrate containing TFe grade of 58.67% and Fe recovery of 57.82% was obtained. Li et al. [25] carried out reduction roasting of iron tailings with Fe grade 13.53% using CO and recovered iron mineral by a low-intensity magnetic separation process. Iron concentrate with a TFe grade of 67.09% and Fe recovery of 85.93% was obtained, which was suitable for blast furnace production.

As evidenced by practice, magnetization roasting combined with the magnetic separation process is one of the most promising methods for the recovery of refractory iron ores. And the pre-enrichment suspended magnetization roasting, and magnetic separation technology (PSRM) is one of the most mature magnetization roasting technologies at present [26,27]. Conventional magnetization roasting processes (shaft furnace, rotary kiln, boiling furnace) have problems, such as high energy consumption, over-reduction, and under-reduction phenomena, which lead to poor sorting index of their roasted products. The PSMR technology has the advantages of high mass-heat transfer efficiency, low reaction temperature, short reaction time, uniform product quality, and a good sorting index. Meanwhile, the energy consumption of PSMR technology is about 30% lower than that of conventional roasting per ton of concentrate [28].

For a fine-grained complex hematite ore (from Anshan, Liaoning Province) with a low separation index, the single-factor and orthogonal experiments were first conducted for the pre-enrichment and reverse flotation process (PRF). Under the optimum conditions, a flotation concentrate was obtained with a Fe grade of 65.89%, but the Fe recovery was only 52.47%. Iron recovery still has great potential from the fine-grained complex hematite ore.

In this work, the fine-grained complex hematite ore was processed and purified using PSRM. The effects of different experimental conditions on the recovery of iron minerals from fine-grained complex hematite ore were investigated. Firstly, the pre-enriched concentrate with optimal pre-enrichment conditions was used as the roasting feed ore, and the regulation mechanism of different influencing factors on the suspension magnetization roasting was investigated. The Fe grade and Fe recovery of concentrate were directly characterized by the magnetic separation to optimize the roasting conditions. The chemical component, phase, crystal structure, magnetic performance, and microstructure changes of products were detected by the chemical analysis, X-ray diffraction (XRD), X-ray photoelectron spectroscopy (XPS), vibrating sample magnetometer (VSM), scanning electron microscope (SEM), Brunauer-Emmett-Teller (BET) and other analytical methods.

MATERIALS AND METHODS

1. Materials

Fine-grained complex hematite ore was provided from Liaoning Province, China. The major chemical composition is shown in Table 1, which reports a mining ore with low-grades of iron (TFe: 21.18%). The mass content less than 0.074 mm in the sample accounts for 32.31%. Table 2 indicates the iron phase composition in the sample, which reveals the percentage of hematite accounting for 82.64%, magnetite 0.69%, and iron-bearing silicate 12.05%. Fig. 1 shows the XRD pattern of the sample, which exhibits the main iron minerals are hematite, magnetite, and limonite, and the gangue is mainly quartz.

Hematite and magnetite were used as the main valuable minerals in the samples. Mineral dissemination and grain size distribution of samples were determined in Fig. 2 and Fig. 3. The particle size distribution of hematite and magnetite is extremely fine, with 48.28% of mineral grains smaller than 0.074 mm.

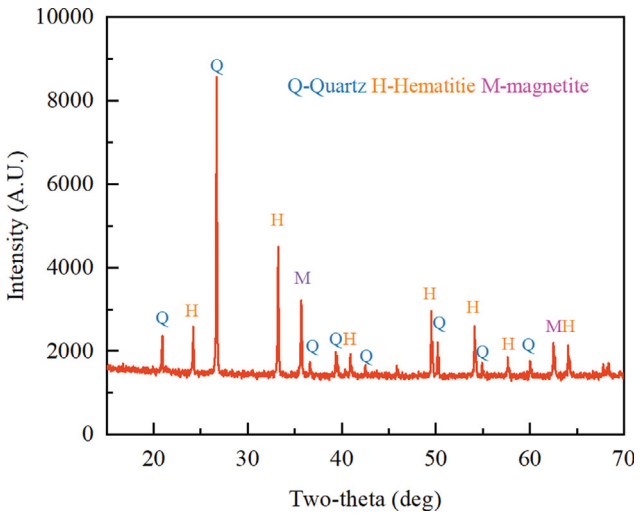

Fig. 1. The XRD pattern of the sample.

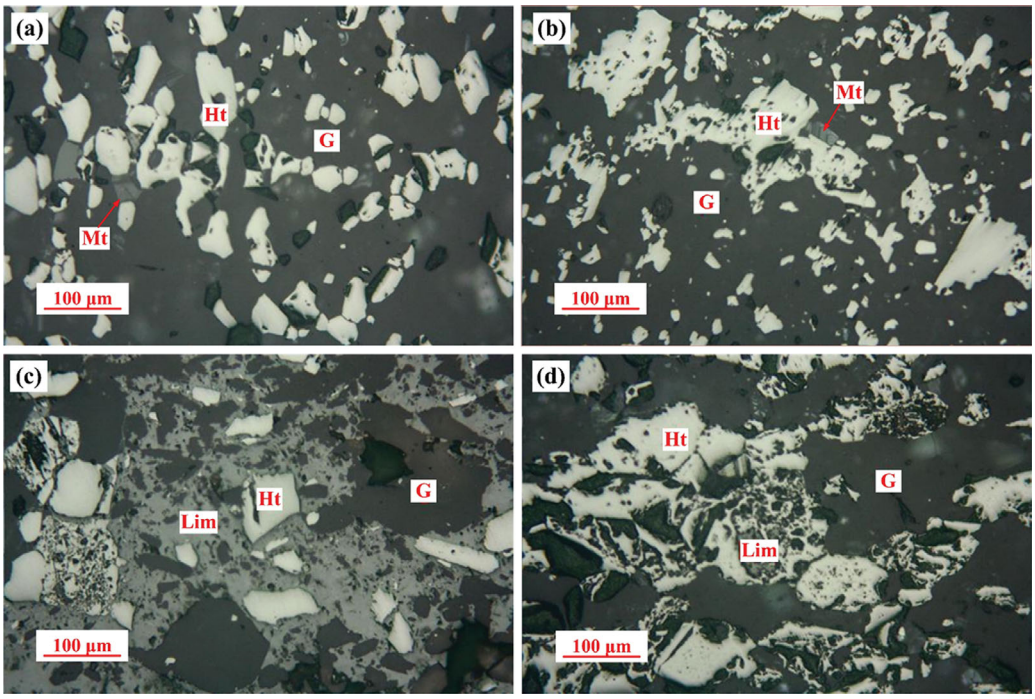

Fig. 2. Microscopic image of the original sample (Ht-hematite; Mt-magnetite; Lim-limonite; G-quartz).

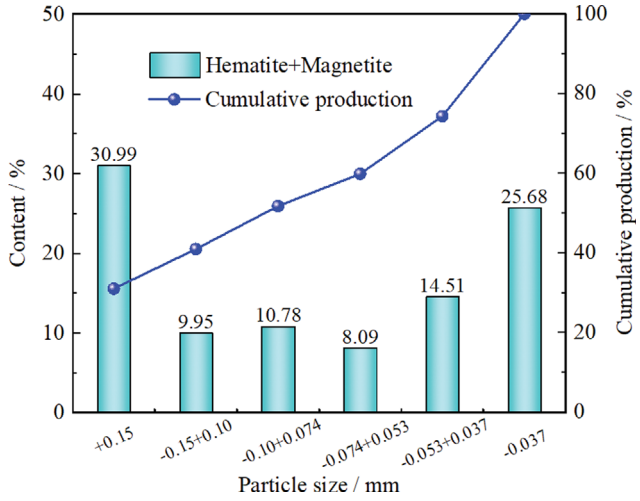

Fig. 3. Grain size distribution of useful minerals (hematite+magnetite) in the sample.

In the roasting test, N_2 (99.9%) and CO (99.9%) were used as inert gases and reductant gases, respectively.

2. Methods and Equipment

The experimental system of the PSRM is shown in Fig. 4. The quality of the iron ore will affect the subsequent process capacity. So, numerous pre-enrichment experiments were conducted to improve the Fe grade of the ore. According to the distribution characteristics of iron minerals in the sample, the pre-enrichment experiments (including grinding fineness and magnetic field strength) were first performed, and the conditions of the experiment are shown in Table 3. The pre-enrichment experiment indicated that the best pre-enrichment concentrate with 52.59% Fe grade and 79.79% Fe recovery could be obtained when grinding fineness was 92.11% under the order of −0.040 mm and magnetic field intensity was 5,000 Oe. The pre-enrichment tailing with a yield of 69.55% and Fe grade of 6.21% could be thrown by the pre-enrichment process, thus improving the efficiency of subsequent operation. Therefore, the pre-enrichment concentrate was used as the roasting feed for suspension magnetization roasting.

Suspension magnetization roasting experiments were conducted in a small vertical suspension furnace (OTF-1200X-S-VT, HFKJ, China). The roasting feed (22 g) was reduced at roasting temperature (400-600 °C), roasting time (0-20 min), reductant concentra-

Table 3. Conditions of pre-enrichment experiments

Project	Grind fineness	Magnetic field intensity (Oe)
Grinding fineness experiments	60, 70, 80, 90, and 95% passing 0.074 mm	6,000
	85, 90, and 95% passing 0.045 mm	6,000
	86.47, 92.11, and 95% passing 0.040 mm	6,000
Magnetic field intensity experiments	92.11% passing 0.040 mm	4,000, 5,000, 6,000, 7,000, and 8,000
	95% passing 0.038 mm	5,000

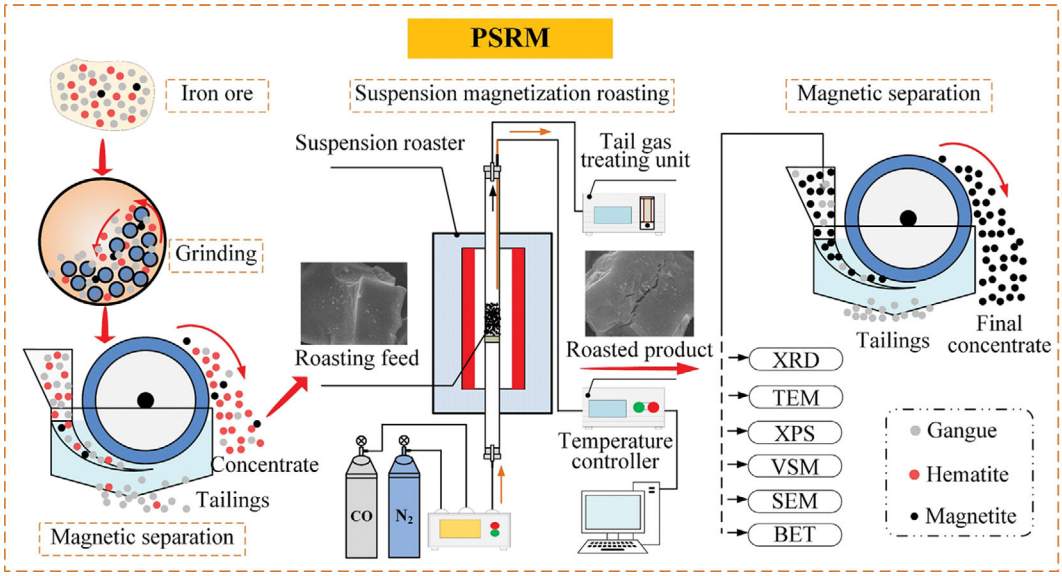

Fig. 4. Test system of the PSRM.

Table 4. Reduction reaction of flotation tailings under suspension magnetization roasting [3,29]

Equation	Reactions
1	$Fe_2O_3(s)+1/3CO(g)=2/3Fe_3O_4(s)+1/3CO_2(g)$
2	$Fe_3O_4(s)+CO(g)=3FeO(s)+CO_2(g)$
3	$Fe_3O_4(s)+4CO(g)=3Fe(s)+4CO_2(g)$
4	$FeO(s)+CO(g)=Fe(s)+CO_2(g)$

tion (10-50%), and total gas flow (100-500 ml). After the experiment, the remaining gas in the furnace was purged using N_2, and the roasted products were cooled to room temperature (25 °C) under the N_2 atmosphere. Then, the roasted products were separated by a Davis Tube Tester (XCGS-50) and the magnetic field intensity was 104 k·Am^{-1}. Table 4 shows the main chemical reactions of iron minerals during suspension magnetization roasting.

3. Characterization Methods

The X-ray diffraction analysis of samples was by XRD (X' Pert PRO MPD) with Cu Kα radiation with 40 kV and 40 mA, respectively. The diffraction angle range (2θ) was from 15° to 70° and 12°/min. The Fe phase compositions of different stages products were characterized according to the iron chemical phase analysis [25]. Mineral dissemination and grain size distribution of samples were analyzed by optical microscopy (BX41M, Olympus Optical, Japan). The crystal structure of the sample was determined by the TEM (G20, FEI, American) instrument. The XPS of samples were observed by Thermo Scientific ESCALAB 250Xi using an Al Kα X-ray source (1,486.6 eV), and the results were processed using AVANTAGE software (version 5.974). The magnetic performance analysis of samples was analyzed via the vibratory sample magnetometer (VSM, Model 7410, Lake Shore, Columbus, Ohio, USA). The microstructure characterization of samples was determined using a scanning electron microscope (SSX550 SEM, Shimadzu, Japan) and an automatic dynamic N_2 adsorption specific surface area analyzer (3H-200BET-A, BeiShiDe, China).

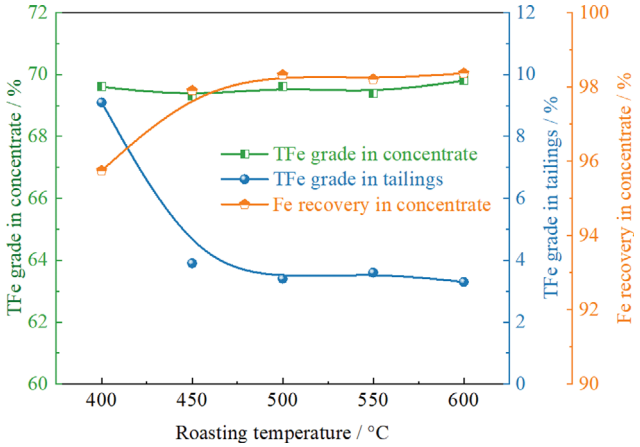

Fig. 5. Effect of the roasting temperature on separation indexes.

RESULTS AND DISCUSSION

1. Magnetization Suspension Roasting and Magnetic Separation

1-1. Effect of Roasting Temperature

Fig. 5 shows the effect of roasting temperature on separation indexes and the other conditions are a roasting time of 12 min, a reductant concentration of 20%, and a total gas flow of 300 mL/min.

As can be seen from Fig. 5, the roasting temperature had a major effect on the Fe recovery and Fe grade in tailings, but little effect on Fe grade in concentrate. When the range of roasting temperature was from 400 °C to 600 °C, the Fe grade in concentrate remained at approximately 69.5%. However, the Fe recovery and Fe grade in tailings significantly varied from 74.61% and 9.10% at 400 °C to 98.32% and 3.40% at 500 °C, respectively. According to the thermodynamic analysis, increasing the roasting temperature could improve the reaction rate (as Eq. (1)), and promote the conversion of hematite to magnetite, which could easily recover by magnetic sepa-

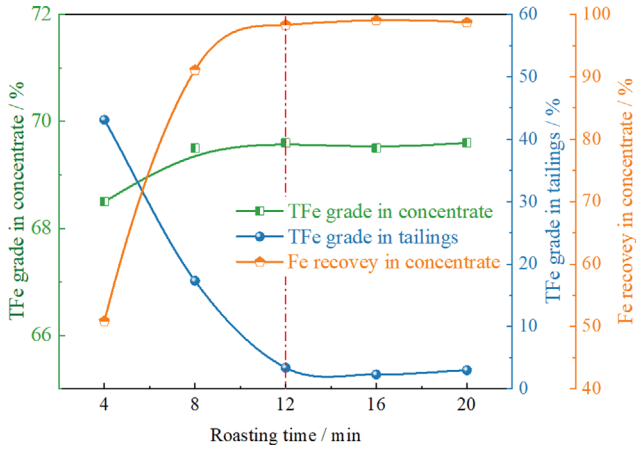

Fig. 6. Effect of the roasting time on separation indexes.

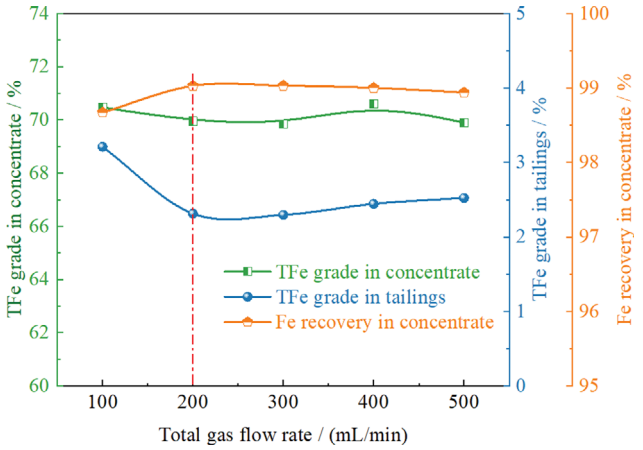

Fig. 8. Effect of the total gas flow on separation indexes.

ration. However, a significant change in the Fe recovery and Fe grade in tailings was not obtained when the roasting temperature was increased from 500 °C to 600 °C. Thus, 500 °C was selected as the best roasting temperature in the following work.

1-2. Effect of Roasting Time

Fig. 6 exhibits the effect of roasting time on the separation indexes. The roasting temperature was 500 °C, the reductant concentration was 20%, and the total gas flow was 300 mL/min.

When the roasting time was 4 min, Fe grade and Fe recovery in concentrate, and Fe grade in tailings were 68.50%, 50.84%, and 43.10%, respectively. Significant improvement of Fe grade and Fe recovery in concentrate of 69.50% and 99.05% was obtained when the roasting time was further increased to12 min. Meanwhile, the Fe grade in tailings had decreased sharply to 2.30%. However, the Fe grade and Fe recovery in concentrate, and Fe grade in tailings were stable when the roasting time was further increased to 20 min. If the roasting time is too long, magnetite is prone to over-reduction reactions (Eq. (2)-(4)), which harms the separation indexes. Therefore, the roasting time of 12 min was applied as a suitable time.

1-3. Effect of Reductant Concentration

Fig. 7 reveals the effect of reductant concentration on the separation indexes. The roasting temperature was 500 °C, the roasting time was 12 min, and the total gas flow was 300 mL/min. Fig. 7 shows that Fe grade in concentrate fluctuated around 69.5% as the reductant concentration increased from 10% to 50%. Reductant concentration had a significant effect on Fe grade in tailings and Fe recovery in concentrate. The Fe grade in tailings was decreased from 6.60% to 2.90%, and Fe recovery in concentrate was increased from 54.39% to 99.58%, with the reductant concentration increased from 10% to 30%. This is because the increase of the reductant concentration may increase the probability of collision of the reductant (CO) and solid phases, which may accelerate the magnetization roasting reaction process (Eq. (1)). Therefore, the reductant concentration of 30% was chosen as the reductant concentration for magnetization roasting.

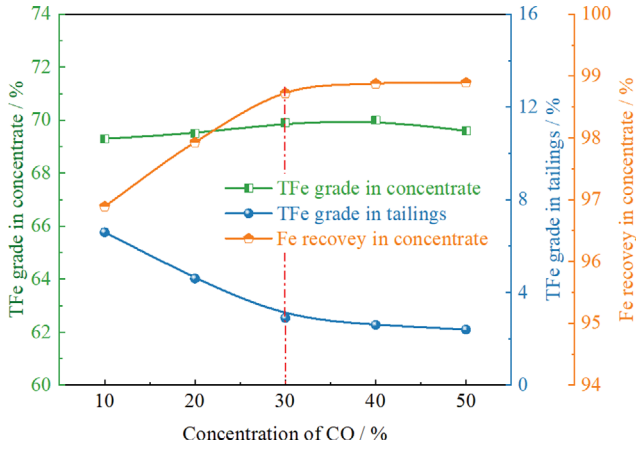

Fig. 7. Effect of the reductant concentration on separation indexes.

1-4. Effect of Total Gas Flow

Fig. 8 presents the effects of the total gas flow on the separation indexes. The roasting temperature was 500 °C, the roasting time was 12 min, and the reductant concentration 30%.

Fig. 8 shows the effect of total gas flow on the separation indexes. As the total gas flow increased from 100 mL/min to 200 mL/min, the Fe recovery increased from 98.67% to 99.03%, and the Fe grade in tailings hit the rock bottom at 2.31%. Additionally, a larger total gas flow could provide more reductants and cause higher collision opportunities. However, when the total gas flow was further increased to 500 mL/min, the separation indexes were relatively stable. In general, the influence of total gas flow on the separation indexes was less than other factors, and it had a relatively large operating range under the excellent separation indexes.

In summary, Fe grade of 69.96%, Fe recovery of 99.03% in iron concentrate, and Fe grade of 2.31% in tailings can be obtained under conditions of a roasting temperature of 500 °C, roasting time was 12 min, reductant concentration of 30%, and total gas flow of 200 mL/min.

2. Phase Transformation Mechanism

2-1. Phase Selective Transition Analysis

The phase transformations were estimated by X-ray diffraction and the iron chemical phase analysis. The change in X-ray diffraction patterns of the roasted products as the roasting time was presented at 500 °C in Fig. 9. The iron phase composition of products at different stages is shown in Fig. 10.

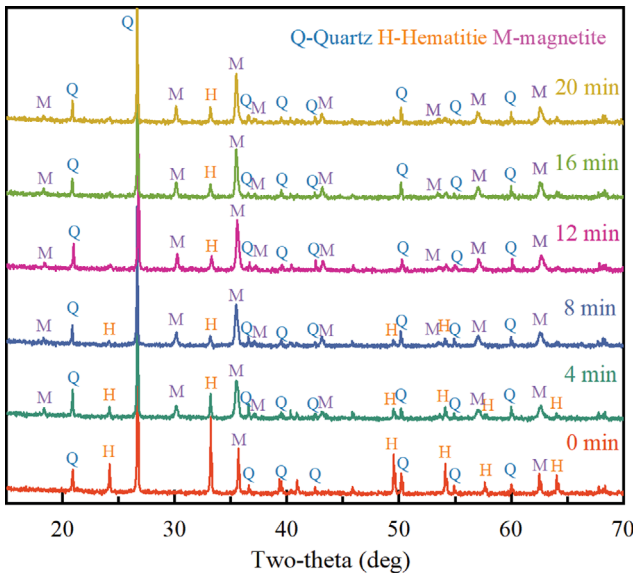

Fig. 9. XRD patterns of products at different times.

Fig. 9 show that new diffraction peaks emerged at 18.3°, 30.1°, 37.1°, 43.1°, and 57.0° when roasted at 500 °C for 4 min, corresponding to 102, 114, 204, 220, 232 crystal planes of the magnetite structure, respectively. With the roasting time increasing, the hematite was gradually converted to magnetite. When the roasting temperature was 12 min, the hematite characteristic peaks 012, 024, 116, 122, and 300 disappeared in the roasted product. When the roasting time exceeded 12 min, the hematite characteristic peak (104) still existed in the roasted product. XRD results demonstrated that the hematite in the sample was gradually reduced to magnetite with the prolonging of roasting time [31]. Meanwhile, the increase in magnetite content is conducive to improving the efficiency of magnetic separation.

The iron phase composition of products at different stages was quantitatively analyzed via the chemical iron phase method. Fig. 10(a) shows the roasted feed was mainly composed of hematite (TFe grade=45.86%) and magnetite (TFe grade=3.11%). After roasting, the TFe grade in magnetite increased from 3.11% in the roasted feed to 53.36% in the roasted product, and that further increased to 69.37% by magnetic separation. Simultaneously, the TFe grade in hematite decreased from 45.86% in the roasted feed to 0.35% in the roasted product. Also, Fig. 10(b) shows that the Fe content in magnetite accounted for 99.16% of TFe in magnetic concentrate. Finally, the TFe grade of tailings was only 2.31%, mainly in the form of hematite, magnetite, and Ferric metasilicate, whose Fe content was 54.11%, 30.30%, and 12.55%, respectively. In short, the hematite in the roasted feed was almost completely reduced to magnetite.

2-2. Transmission Electron Microscopy Characterization

In the magnetization roasting, the phase transformation caused by hematite reduction will lead to a crystal structure change of the particles. High-resolution transmission electron microscopy (HRTEM) was used to characterize the particles before and after magnetization roasting. The roasting feed (Fig. 11(b)) showed the characteristic spacings of 0.2516 nm, 0.2699 nm, and 0.3779 nm for the 110, 104, and 102 lattice planes of hematite. As shown in Fig. 11(d), the lattice fringes of the roasted product display interplanar spacings of 0.2528 nm, 0.2964 nm, and 0.4841 nm in the particle, which match well, respectively, with those of the 311, 220, and 111 planes of the magnetite. TEM results confirmed that hematite was transformed into magnetite with a spinel structure with good crystallinity. It is consistent with the results of XRD and iron chemical phase analysis.

2-3. X-ray Photoelectron Spectroscopy Analysis

To further verify the results of phase transition studies, XPS analyses on the products at different stages were conducted. The atomic composition of the product's surface at different stages is listed in

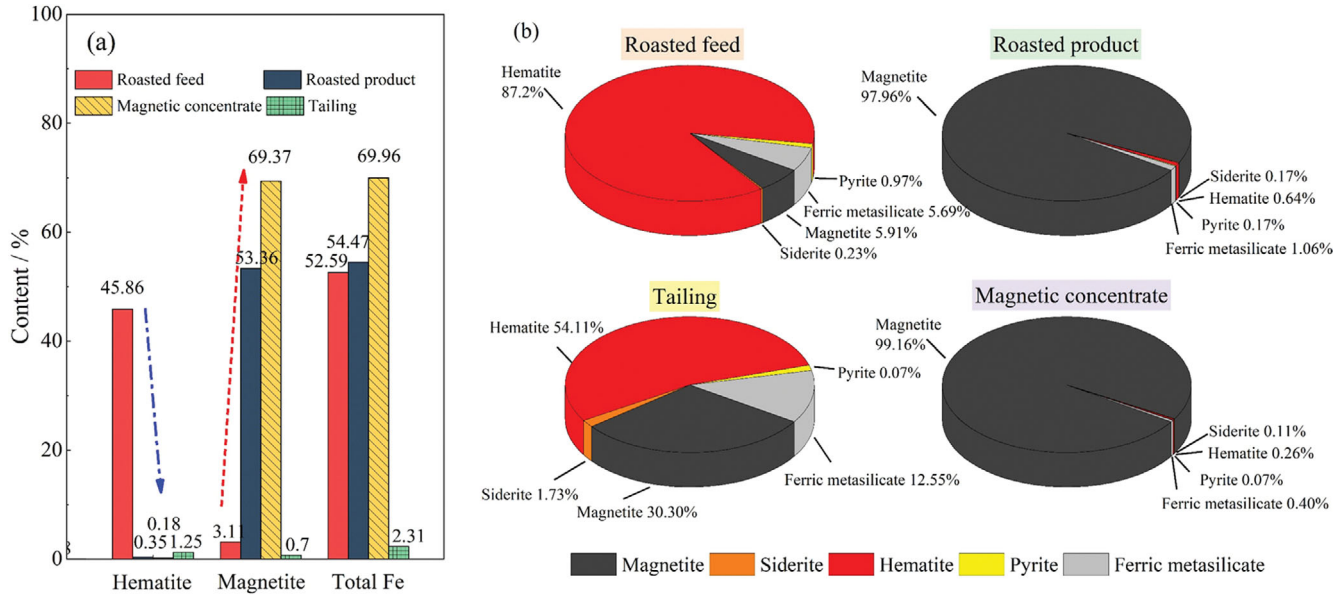

Fig. 10. The iron phase composition of products at different stages: (a) Fe content in the different iron minerals; (b) percentage of iron phase at different stages.

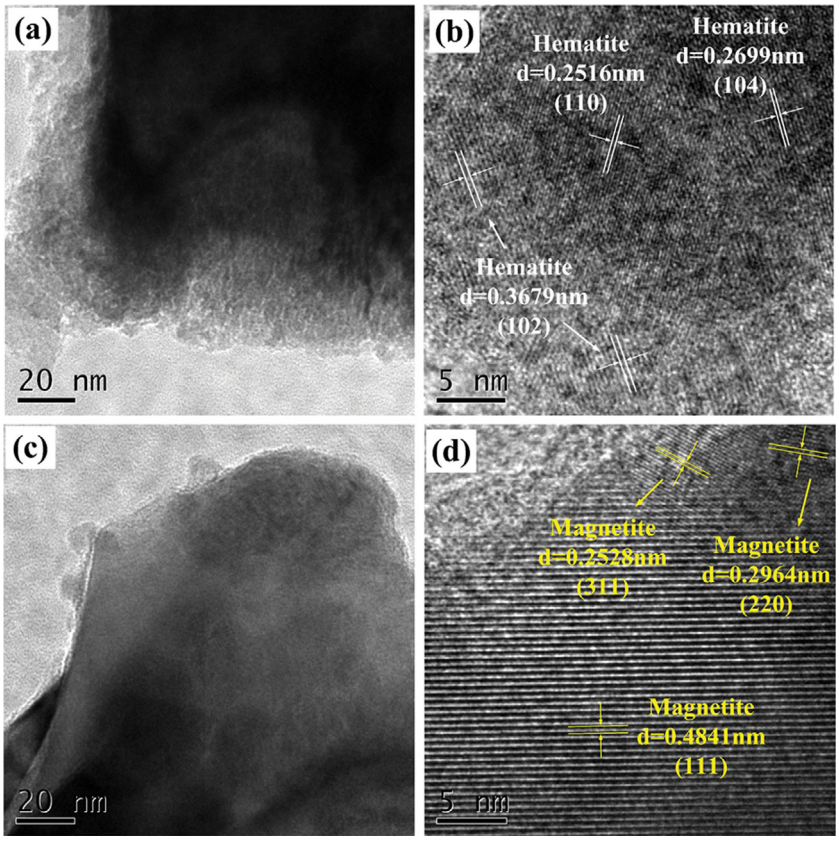

Fig. 11. High-resolution TEM (HRTEM) images for (a), (b) Roasting feed and (c), (d) Roasted product.

Table 5. The atomic concentration of elements for the products surface is determined by XPS

Samples	The atomic concentration of elements (atomic %)			
	Fe	Si	O	C
Roasting feed	8.63	14.61	49.39	27.37
Roasted product	9.31	15.31	48.96	26.43
Magnetic concentrate	15.5	7.88	46.43	30.2
Tailings	2.31	22.5	47.57	27.63

Table 5. The results show that the atomic concentration of Fe increased and that of O decreased after magnetization roasting. While after magnetic separation, the atomic concentration of Fe increased in magnetic concentrates and that of Fe significantly decreased in tailings, which confirmed that roasted product has excellent separation results.

High-resolution XPS spectra of Fe2p for products at different stages are exhibited in Fig. 12. Fig. 12 shows the valence states of Fe in these four products. The Fe2p spectrum of roasting feed contained two peaks (Fig. 12(a)), $Fe2p_{3/2}$ and $Fe2p_{1/2}$, which are 710.80 eV and 724.30 eV at binding energy. The two photoelectron peaks were attributed to Fe^{3+} of iron oxide. Meanwhile, low binding energy appeared at a low-intensity peak, which was Fe^{2+} ion with a low oxidation state. The results show that there were iron oxides (magnetite) containing Fe^{3+} and Fe^{2+} in the roasted feed, and the results

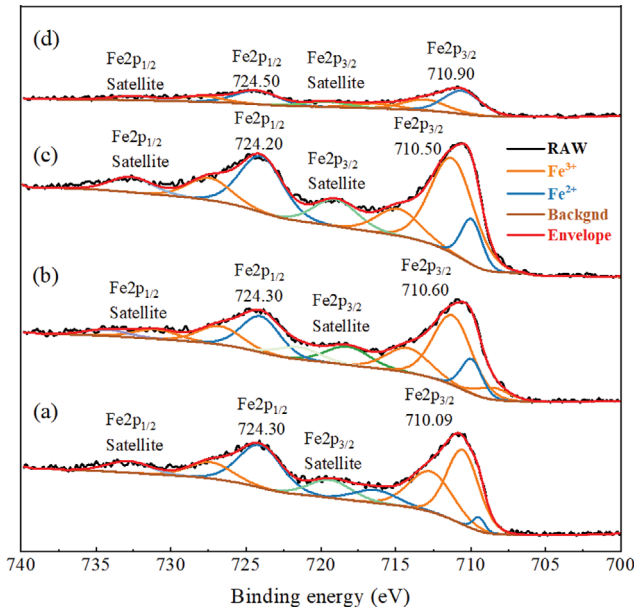

Fig. 12. High-resolution XPS spectra of Fe2p for (a) Roasting feed, (b) Roasted product, (c) Magnetic concentrate, (d) Tailings.

are consistent with the analysis of the iron phase. For the roasted product (Fig. 12(b)), the intensity of the Fe^{2+} peak increased, indicating that the roasting reaction led to the reduction of Fe^{3+} state to Fe^{2+} state, and the magnetite content in the roasted product in-

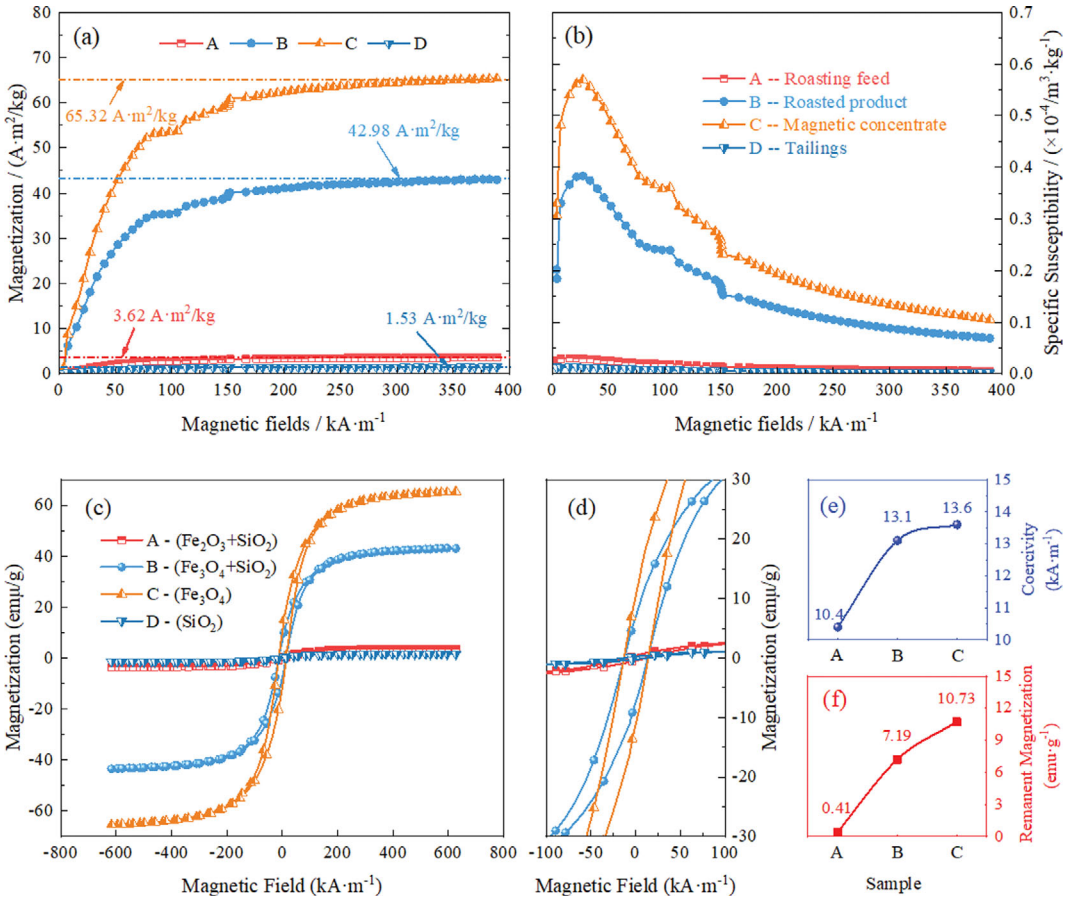

Fig. 13. The magnetic analysis of products: (a) magnetization; (b) specific susceptibility; (c)-(d) hysteresis loop; (e) Coercivity; (f) Remanent magnetization.

creased at the same time. Figs. 12(c) and 12(d) show that the peak intensity of Fe2p spectra in the magnetic concentrate was greater than that in the roasting products and tailings. It confirms that magnetite was further enriched into the magnetic concentrate via magnetic separation. The XPS results also provide reliable evidence for the transformation process of hematite to magnetite.

2-4. Magnetic Performance Analysis

The magnetic of the product is proportional to the conversion fraction of hematite to magnetite [30]. Since the roasting feeding was weak magnetic properties, an increase in saturation magnetization indicated that Fe_2O_3 transformed to Fe_3O_4 in the roasted product. So the higher the Fe_3O_4 content, the higher the saturation magnetization. The magnetic analysis of products is in Fig. 13.

Fig. 13(a) indicates that saturation magnetization increased from 3.62 $Am^2 \cdot kg^{-1}$ in the roasting feed to 42.98 $Am^2 \cdot kg^{-1}$ in the roasted product and further increased to 65.32 $Am^2 \cdot kg^{-1}$ by magnetic separation. It indicates that the magnetite content greatly increased after roasting, and magnetite was enriched again via magnetic separation. The results were consistent with the iron phase composition analysis. Meanwhile, the coercivity and residual magnetization of the products had similar trends, increasing from 10.3 $kA \cdot m^{-1}$ and 0.41 $Am^2 \cdot kg^{-1}$ in roasting product to 13.1 $kA \cdot m^{-1}$ and 7.19 $Am^2 \cdot kg^{-1}$ in the roasted product, respectively. Finally, the saturation magnetization, coercivity, and residual magnetization of magnetic concentrate were 65.32 $Am^2 \cdot kg^{-1}$, 13.6 $kA \cdot m^{-1}$, and 10.73 $Am^2 \cdot kg^{-1}$, respectively The results show that hematite could be reduced to magnetite via suspension roasting, and iron minerals in roasted products can be enriched efficiently by low-intensity magnetic separation.

2-5. Microstructure Characterization

To study the effect of suspension magnetization roasting on the microstructure of products, scanning electron microscope analysis (SEM) and BET analysis were performed on the roasting feed and roasted products.

Fig. 14 presents SEM images of the products. The particles of roasting feed show a microscopic structure of an angular and smooth surface, without cracks and pores. And a large number of fine particles are also adsorbed on the surface of the particles. During suspension magnetization roasting, iron minerals and quartz underwent heat treatment in a reducing atmosphere, but only hematite reacted and was reduced to magnetite, as shown in Eq. (1). Figs. 14(c) and 14(d) show numerous pores and cracks on the surface of the roasted particles. The particle structure of iron minerals was destroyed by reduction roasting. This is due to the change in the crystal structure of the mineral caused by phase transitions. The generation of pores and microcracks contributed to reducing the difficulty of internal diffusion for CO and CO_2 within the iron ore particles [28]. It also improved the reaction efficiency for the conversion of hematite to magnetite. Besides, the particles covered with pores and cracks

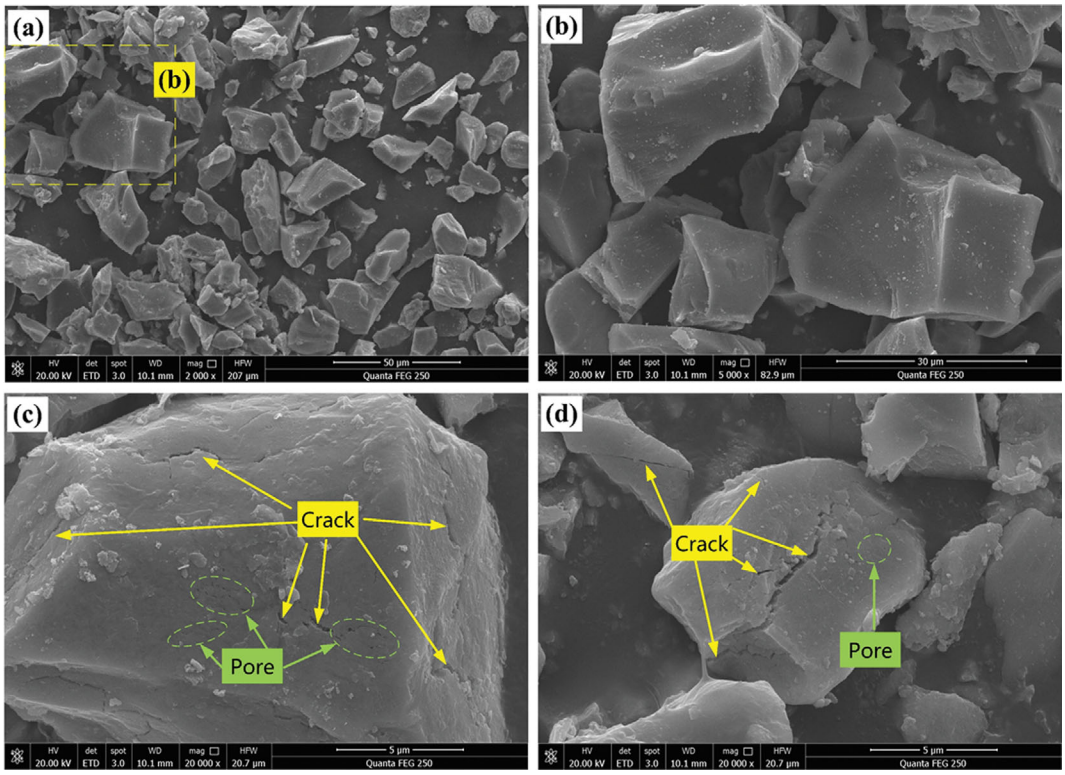

Fig. 14. SEM (a)-(b) Roasting feed, (c)-(d) Roasted product (500 °C, 20 min).

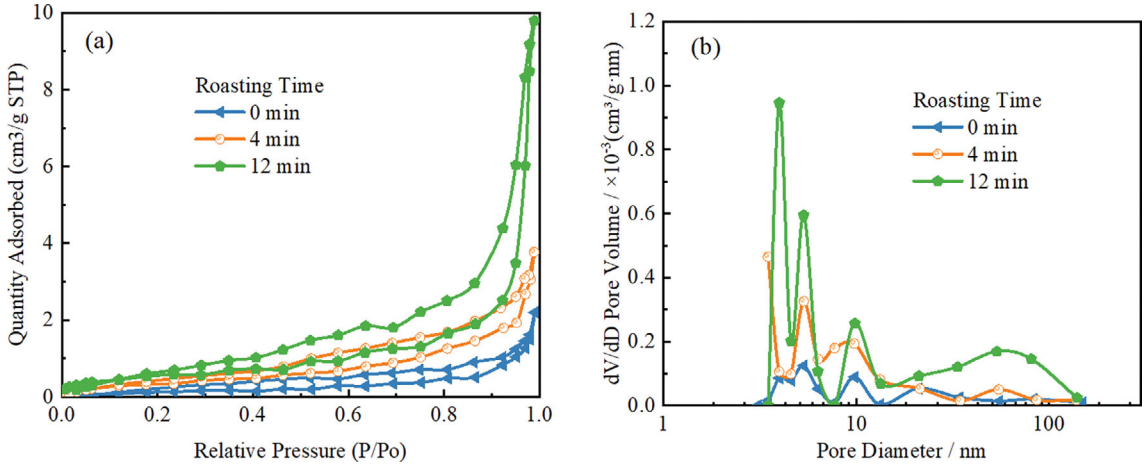

Fig. 15. (a) Isothermal adsorption curve; (b) Characteristics of micropore distribution.

would facilitate subsequent grinding and low-intensity magnetic separation, promoting the efficient recovery of iron minerals.

Fig. 15 demonstrates that the adsorption isotherms belong to the III type. The adsorption of samples in the low-pressure region (P/P_0=0-0.4) was small and without inflection; the adsorption of samples increased at higher relative pressures. It indicates that the ore particles adsorption was mainly a weak gas-solid interaction. The results of BET analysis reveal the effect of magnetization roasting on the pore structure parameters, as shown in Table 6. The specific surface area, pore volume, and average pore diameter of the ore particles increased significantly from 0.496 m^2/g, 0.004 cm^3/g, and 3.493 nm in roasting feed to 2.031 m^2/g, 0.015 cm^3/g, and 3.990 nm in the roasted product (12 min). This is consistent with the

Table 6. Pore structure parameters of ore particles at different roasting times (500 °C)

Roasting time	BET surface area (m^2/g)	Pore volume (cm^3/g)	Average pore diameter (nm)
0 min	0.496	0.004	3.493
4 min	1.252	0.006	3.989
12 min	2.031	0.015	3.990

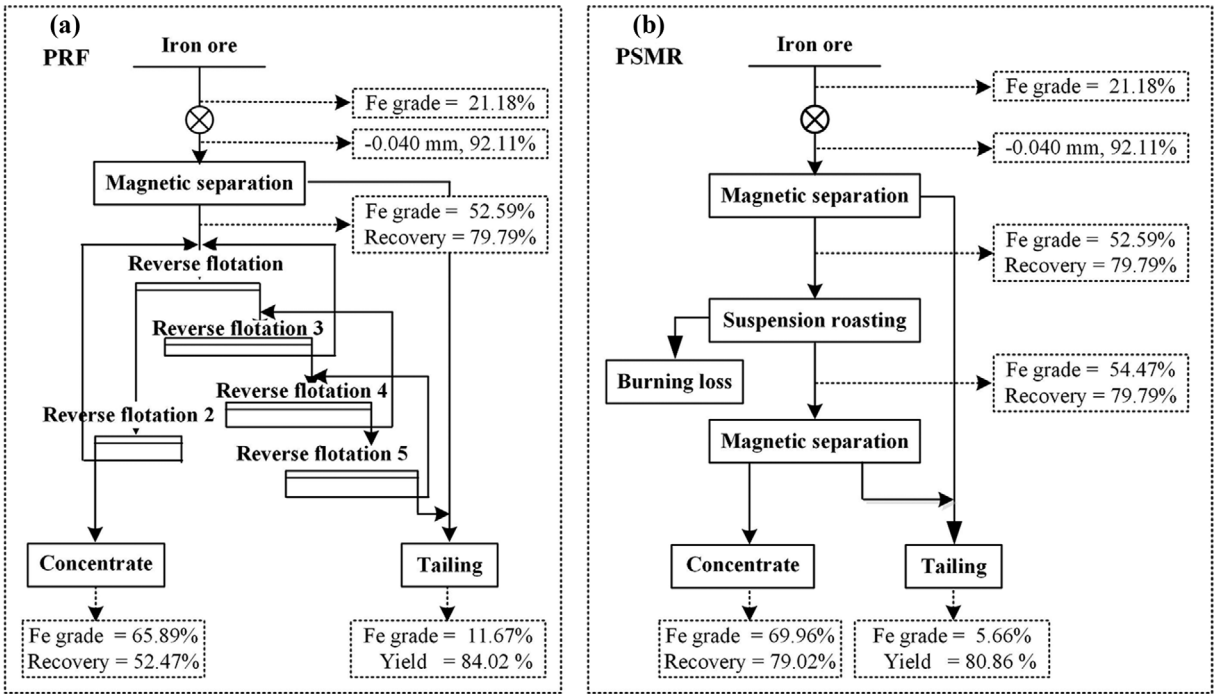

Fig. 16. Flow chart: (a) PRF technology; (b) PSRM technology.

results of SEM analysis.

3. Discussion of Technology Innovation

Fig. 16 illustrates the full process of iron extraction from iron ore by the PRF and PSRM techniques. The flotation conditions (including collector, depressing agent, and conditioning agent) in PRF were optimized with single factor and orthogonal experiments under the best pre-enrichment conditions. Flotation concentrate was obtained with a Fe grade of 65.89% and a Fe recovery of 52.47%. Compared with the PRF, the Fe grade of concentrate obtained by the PSRM increased by 4.07%, the Fe recovery increased by 26.55%, and the Fe grade of final tailings decreased by 6.01%. Therefore, the production of Fe can be increased by 50.60% without increasing raw materials.

PSRM technology can simplify and shorten the beneficiation process, and significantly improve Fe grade and recovery in concentrate. It can realize the efficient utilization of resources and has good social and environmental benefits.

CONCLUSIONS

Major valuable compositions of fine-grained complex hematite ore were hematite, magnetite, and limonite. Most iron minerals and quartz were fine-disseminated together, which were hard to be separated. An innovative and efficient method of Fe extraction from fine-grained complex hematite ore was proposed in this work. Roasting temperature, roasting time, reductant concentration, and total gas flow were the main factors that affect Fe recovery. The magnetic concentrate with Fe grade of 69.96% and Fe recovery rate of 79.02% occurred under the following conditions: roasting temperature of 500 °C, roasting time of 12 min, reductant concentration of 30%, and total gas flow of 200 mL/min. Meanwhile, the TFe grade of final tailings was 5.66%. During the suspension roasting process, the hematite and limonite phases were transformed into magnetite. After roasting, TFe grade in magnetite increased from 3.11% in the roasted feed to 53.36% in the roasted product, and that further increased to 69.37% by magnetic separation. The iron phase transition destroyed the structure of the crystal structure of the mineral, but the numerous pores and microcracks enhanced the internal diffusion process of CO and CO_2 in the iron ore particles. It also improved the reaction efficiency for the conversion of hematite to magnetite. The results indicate that the effective utilization of fine-grained complex hematite ore using PSRM is technically viable.

ACKNOWLEDGEMENTS

The authors are extremely grateful for the financial support received from the National Natural Science Foundation of China (Grant Nos. 51734005 and 51904058), the Fundamental Research Funds for the Central Universities (N2101023), and the Open Foundation of State Key Laboratory of Mineral Processing (Grant No. BGRIMM-KJSKL-2020-17).

REFERENCES

1. S. Patra, A. Pattanaik and V. Rayasam, *Can Metall Q.*, **58**, 28 (2019).
2. J. W. Yu, Y. X. Han, Y. J. Li, P. Gao and Y. S. Sun, *Sep. Sci. Technol.*, **52**, 1768 (2017).
3. Y. S. Sun, X. L. Zhang, Y. X. Han and Y. J. Li, *Powder Technol.*, **361**, 571 (2020).
4. D. Komljenovic, L. Stojanovic, V. Malbasic and A. Lukic, *Int. J. Min. Sci. Technol.*, **30**, 737 (2020).

5. Z. Y. Lan, Z. N. Lai, Y. X. Zheng, J. F. Lv, J. Pang, J. L. Ning, *J. Cent. South Univ.*, **27**, 37 (2020).
6. J. W. Yu, Y. X. Han, P. Gao, Y. J. Li, S. Yuan and W. B. Li, *Physicochem. Probl. Mineral Pro.*, **54**, 668 (2018).
7. G. B. Abaka-Wood, M. Zanin, J. Addai-Mensah and W. Skinner, *Miner. Eng.*, **142**, 105888 (2019).
8. J. He, L. Zhu, X. Bu, C. Liu, Z. Luo and Y. Yao, *Chem. Eng. Process.*, **138**, 27 (2019).
9. R. M. F. Lima and F. D. V. F. Abreu, *J. Mater. Res. Technol-JMRT*, **9**, 2021 (2020).
10. W.-w. Wang and Z.-y. Li, *Miner. Eng.*, **155**, 106453 (2020).
11. E. Matiolo, H. J. B. Couto, N. Lima, K. Silva and A. S. de Freitas, *Miner. Eng.*, **158**, 106608 (2020).
12. W. Li, L. Zhou, Y. Han, Y. Zhu and Y. Li, *Powder Technol.*, **343**, 270 (2019).
13. J. F. He, C. G. Liu, J. Q. Xie, P. Hong and Y. K. Yao, *Powder Technol.*, **319**, 346 (2017).
14. Y. Yao, Q. Bai, J. He, L. Zhu, K. Zhou and Y. Zhao, *Waste Manage.*, **103**, 218 (2020).
15. Z. Gao, X. Chai, E. Zhou, Y. Jia, C. Duan and L. Tang, *Int. J. Min. Sci. Technol.*, **30**, 883 (2020).
16. S. S. Rath, H. Sahoo, N. Dhawan, D. S. Rao, B. Das and B. K. Mishra, *Sep. Sci. Technol.*, **49**, 1927 (2014).
17. F. F. Wu, Z. F. Cao, S. Wang and H. Zhong, *J. Alloy. Compd.*, **722**, 651 (2017).
18. S. D. Lu, S. H. Ju, J. H. Peng and X. P. Zhu, *High Temp. Mater. Process.*, **34**, 147 (2015).
19. C. Xu, H. W. Cheng, G. S. Li, C. Y. Lu, X. G. Lu, X. L. Zou and Q. Xu, *Int. J. Miner. Metall. Mater.*, **24**, 377 (2017).
20. Z. D. Tang, P. Gao, Y. X. Han and W. Guo, *J. Min. Metall. Sect. B-Metall.*, **55**, 295 (2019).
21. E. Donskoi, A. F. Collings, A. Poliakov and W. J. Bruckard, *Int. J. Miner. Process.*, **114**, 80 (2012).
22. W. Zhou, Y. Sun, Y. Han, P. Gao and Y. Li, *Miner. Eng.*, **164**, 106851 (2021).
23. Y. Qin, Y. Han, P. Gao, Y. Li and S. Yuan, *Miner. Eng.*, **160**, 106662 (2021).
24. Y. S. Sun, X. R. Zhu, Y. X. Han, Y. J. Li and P. Gao, *J. Clean Prod.*, **261**, 121221 (2020).
25. Y. Li, Q. Zhang, S. Yuan and H. Yin, *Powder Technol.*, **379**, 466 (2021).
26. P. Gao, Z. D. Tang, Y. X. Han, E. L. Li and X. L. Zhang, *Powder Technol.*, **343**, 255 (2019).
27. Z. D. Tang, P. Gao, Y. J. Li, Y. X. Han, W. B. Li, S. Butt and Y. H. Zhang, *Powder Technol.*, **361**, 591 (2020).
28. S. Yuan, Q. Zhang, H. Yin and Y. Li, *J. Hazard. Mater.*, **404**, 124067 (2021).
29. H. T. B. M. Petrus, A. D. P. Putera, E. Sugiarto, I. Perdana, I. W. Warmada, F. Nurjaman, W. Astuti and A. T. Mursito, *Miner. Eng.*, **132**, 126 (2019).
30. V. P. Ponomar, N. O. Dudchenko and A. B. Brik, *Miner. Eng.*, **122**, 277 (2018).